# Synaptic Adaptation and Sustained Generation of Waves in a Model of Turtle Visual Cortex

Zachary V. Freudenburg*, Bijoy K. Ghosh, *Fellow, IEEE,* and Philip Ulinski

***Abstract*—Both single and repeated visual stimuli produce waves of activity in the visual cortex of freshwater turtles. Large-scale, biophysically realistic models of the visual cortex capture the basic features of the waves produced by single stimuli. However, these models do not respond to repetitive stimuli due to the presence of a long-lasting hyperpolarization that follows the initial wave. This paper modifies the large-scale model so that it responds to repetitive stimuli by incorporating Hebbian and anti-Hebbian learning rules in synapses in the model. The resulting adaptive model responds to repetitive stimuli with repetitive waves. However, repeated presentation of a stimulus to a restricted region of visual space produces a habituation in the model in the same way it does in the real cortex.**

***Index Terms*—Synaptic Adaptation, Turtle Visual Cortex, Hebbian Learning, Large Scale Cortex Model.**

## I. Introduction

VISUAL stimuli evoke a wave of activity that propagates across the visual cortex of freshwater turtles. The waves have been demonstrated *in vivo* [1], [2], [3] and in a reduced eye-brain preparation using both multielectrode arrays and voltage sensitive dyes [4], [5], [6]. The basic dynamics of the waves are stereotypical: the wave originates near the rostral pole of the cortex and propagates across the cortex to its caudal pole. In most cases, a secondary wave, or reflection, occurs at the caudal pole of the cortex and propagates back into the cortex. However, there are detailed differences in the spatiotemporal dynamics of the wave that can be detected using a variant of principal component analysis. Such analyses demonstrate that information about the positions of stimuli in visual space and the speeds of moving stimuli are encoded in the dynamics of the wave [7]. Propagating waves also occur in large-scale, biophysically realistic models of turtle visual cortex [8], [9]. Emphasis in the models was put on capturing major features of the special distributions of the neurons and geniculate afferents and the physiology of cortical neurons in the cortex that govern the propagation patterns of waves. These models contain approximately 800 cortical neurons and 200 neurons in the dorsal lateral geniculate complex, which form a large enough model to capture the wave features while keeping the computational complexity manageable. Models of each of the four major populations of neurons in the cortex were based on detailed anatomical and physiological data. The geniculate neurons were simple spike generators that provided inputs to the cortical neurons. The spatial distribution of neurons in the cortex, the connections between cortical neurons and the geniculate afferents within the cortex were based on the known anatomy. Simulated light flashes, stationary spots of light, or moving spots of light evoked waves in the model cortex that accurately reproduced the waves seen in real cortices. Analysis using the methods developed with the real cortices showed that waves in the model cortex code information about visual stimuli in the same way as do waves in the real cortex [7].

However, an important discrepancy between the behavior of the real cortex and the model concerns their responses to repeated stimuli. There is evidence from several *in vivo* studies that turtle visual cortex responds to the presentation of repetitive visual stimuli. First, Gusel'nikov and Pivovarov [10] recorded both evoked potentials and intracellular responses from the visual cortex of pond turtles. Stimuli consisting of bars of various shapes and orientations were presented in the contralateral visual field. Repeated presentations of the same stimulus produced both extracellular and intracellular responses that decreased in amplitude with each successive presentation of the same stimulus. However, a strong response could be elicited if the size or orientation of the bar was abruptly changed. These experiments demonstrated a form of habituation that is specific to the stimulus being used. Second, Prechtl and Bullock [11] recorded from turtle visual cortex using an array of microelectrodes. They presented 10 s sequences of relatively dim light flashes at frequencies of 1 Hz to 6 Hz that were followed by a relatively bright stimulus. The cortex responded to each of the dim light flashes, but responded with an enhanced response to the bright flash. Finally, Prechtl and Bullock [12] recorded event related potentials from turtle visual cortex while presenting trains of 8 ms light flashes and found that a distinct, long-lasting omitted stimulus potential occurred following cessation of the stimulus train. All three of these experiments demonstrate that turtle visual cortex shows forms of plasticity that are associated with repetitive stimulation. However, these effects are not seen in the models because wave propagation in the models is followed by a long-lasting hyperpolarization that is mediated by $GABA_B$ receptors and prohibits cortical responses for several hundred ms after the wave has died out.

The models we have studied to date do not include any form

Manuscript received July 30, 2008; revised October 10, 2008. This work was supported in part by the National Science Foundation (NSF) under Grants BIC 0523983, ECS 0323693 and EIA-0218186. *Asterisk indicates corresponding author.*

Z. V. Freudenburg is in the Department of Computer Science and Engineering, Washington University in St. Louis, MO, USA (phone: 314-935-5804; fax: 314-935-7302; e-mail: zvf1@cec.wustl.edu).

B. K. Ghosh is currently the Brooks Regents Professor of Mathematics and Statistics at Texas Tech University, Lubbock, TX, USA (email: bijoy.ghosh@ttu.edu).

P. S. Ulinski is currently Professor Emeritus in Computational Neuroscience at the University of Chicago, Chicago, IL, USA (email: pulinski@uchicago.edu).

of synaptic plasticity and can be called non-adaptive models. The goal of this paper is to modify the non-adaptive large-scale models by including forms of synaptic plasticity that allow the model cortex to respond to repetitive stimuli. Plasticity was implemented in this adaptive model using Hebbian and anti-Hebbian learning rules. Incorporation of these learning rules resulted in a model that does respond to repetitive stimuli. Consistent with the Gusel'nikov and Pivavarov study, the adaptive model habituates to continuous presentation of the same stimulus. The adaptive model also codes information about the positions of stimuli in visual space and the speed and directions of moving stimuli in the same way as do the non-adaptive models.

## II. Large-scale Model

### A. Structure of the Non-adaptive Models

Two versions of a large-scale model of turtle visual cortex have been developed. Both use the Genesis neural simulation software package [13]. Details of the first version are given in Nenadic *et al.* [8]. This model contains two populations of pyramidal cells (lateral pyramidal cells and medial pyramidal cells) and two populations of inhibitory interneurons (stellate cells and horizontal cells). It was used by Du *et al.* [14], [15] in their studies of information coding in the cortex. The second version contains all of the cells in the first version as well as a third population of inhibitory interneurons, the subpial cells [16]. Details of this model are given by Wang *et al.* [9]. The input in both models consists of an array of 201 model neurons in the lateral geniculate nucleus. Figure 1 shows the spatial distribution of cortical and geniculate cells in the large-scale model that includes subpial cells. Visual stimuli are simulated by injecting 12 nA current pulses in all of the geniculate neurons to simulate full field light flashes, in a cluster of geniculate neurons to simulate localized light flashes, or in a sequence of geniculate neurons to simulate a moving spot of light. A Gaussian noise current with a mean of 0 nA and a standard deviation of 4 nA was injected into the soma compartment of each neuron to simulate general synaptic noise in the model.

### B. Synaptic Plasticity in the Adaptive Model

An adaptive version of the large-scale model was developed for this study by adding a mechanism for synaptic plasticity to the synapses between pyramidal cells and between inhibitory cells and pyramidal cells to the non-adaptive models. (No mechanisms for synaptic plasticity were incorporated in the inhibitory synapses between subpial cells and between stellate cells.) The cellular mechanisms that cause changes in synaptic effectiveness in turtle visual cortex are not known, so no attempt was made to model synaptic plasticity at the cellular or molecular levels. Synaptic plasticity was, instead, represented phenomenologically using Hebbian and anti-Hebbian learning rules. The Hebbian learning rule is written as:

$$weight(t) = weight(t - \Delta t) + R[(pre(t)][post(t)]\Delta t \quad (1)$$

where $weight(t)$ is the weight of a synapse at time, $t$, $weight(t - \Delta t)$ is the weight of the synapse at time, $t - \Delta t$,

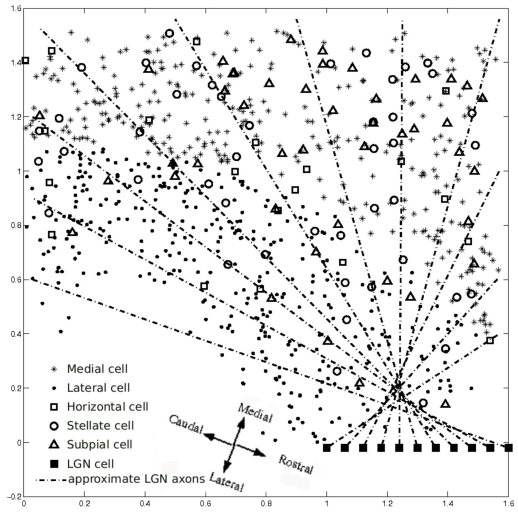


Fig. 1. Distribution of cells the model cortex. This diagram shows the spatial distribution of all of the cells in the model cortex, including subpial cells. Each type of neuron is represented by a different symbol. Representative geniculate neurons are represented by boxes at the lower right edge of the cortex. The trajectories of the axons of the neurons are represented by lines that fan out across the cortex. The scales along the horizontal and vertical axes represent distances in mm.

$\Delta t$ is a differential time step, $t$ is a discrete variable over the modeled time period, $R$ is a constant used to control the modification time scale. The change in synaptic weight, $\Delta w$, for a given time step is

$$\Delta w/\Delta t = R[pre(t)][post(t)]. \quad (2)$$

Changes in synaptic weights are determined by whether or not activity in the presynaptic and postsynaptic cells are synchronous or asynchronous. Synchronous rest will not cause any weight change. Synchronous activity or suppression will cause a weight increase, and asynchronous activity will cause a weight decrease. Anti-Hebbian synaptic modification is achieved by making the rate constant, R, negative. This reverses the sign of the added weight and, thus, reverses the effects of synchronous and asynchronous activities. The adaptation scheme for Hebbian and anti-Hebbbian modification is summarized in Figure 2-A,B. For example, the synaptic weight decreases if the presynaptic cell is hyperpolarized and the postsynaptic cell is depolarized in the Hebbian learning scheme, but increases in the anti-Hebbian learning scheme.

Activity can, in general, be either the spiking rates or the membrane potentials of the cells. In the adaptive model, activity is the membrane potential of the soma compartment of the presynaptic or postsynaptic cell relative to a range of rest values. For example, the upper bound of the postsynaptic rest activity range is set to just below the soma membrane potential at which spiking occurs. The lower bound is set to just below the membrane potential induced by the injected noise current. pre(t) and post(t) are, then, defined as:

$$pre(t) = \begin{array}{c} presynaptic\ activity(t) - \\ nearest\ presynaptic\ rest\ activity\ bound \end{array} \quad (3)$$

$$post(t) = \begin{array}{c} postsynaptic\ activity(t) - \\ nearest\ postsynaptic\ rest\ activity\ bound. \end{array} \quad (4)$$

Activity above the upper bound of the rest level indicates an active (depolarized) cell. Activity between the lower and upper bounds of the rest level indicates the undisturbed state of the cell. Activity below the lower bound of the rest level indicates the suppressed (hyperpolarized) state of the cell.

Responses to repeated stimuli in the non-adaptive models are inhibited by a long-lasting after-hyperpolarization that follows the cessation of a wave. The goal of adding synaptic adaptation to the model is to compensate for this after-hyperpolarization and allow for future wave generation. Since the waves are defined by pyramidal cell activity, the synaptic adaptation scheme can be solely responsive to postsynaptic pyramidal cell activity. Setting the presynaptic rest threshold to a value less than the range of possible presynaptic activity will cause $pre(t)$ to always be positive. Thus, the value of $post(t)$ will control the sign of the weight change and whether the weight is increased or decreased (Fig. 2-C,D). Excitatory AMPA interconnections between pyramidal cells were shown to play a major role in sustaining the cortical wave [9] and are chosen to be anti-Hebbian. This produces increasingly larger synaptic weights between pyramidal cells once the waves have abated and the model enters the after-hyperpolarization phase. On the other hand $GABA_A$ synaptic receptors between inhibitory neurons and pyramidal cells were shown to play a major role in wave cessation [9] and are chosen to be Hebbian. This produces increasingly weaker inhibition of pyramidal cells in response to the after-hyperpolarization phase. The net effect of the connection scheme is that the adaptive model enters a state that favors the generation of additional waves, a pro-activity state, following the cessation phase of an initial wave. Examples of activity in the model and weight states during and after wave propagation are depicted in Figure 3.

The rate constant, $R$, allows for synaptic plasticity on different time scales. A small rate value can be used to model long-term synaptic changes and a large value can be used to model a short-term synaptic adaptation. A negative weight value has no biological significance, so a zero or positive lower weight bound is enforced. An upper weight bound is chosen as twice the non-adaptive synaptic weight value, allowing synapses to essentially double their effectiveness. The weight bounds are modeled as soft bounds that are approached exponentially by modifying $weight(t)$ directly as the weight nears a bound. A zero weight represents an inactive synapse, but a synapse can be reactivated if its presynaptic and postsynaptic cells again become simultaneously active due to other influences. Thus, a zero weight synapse is included for every pair of cells that could become active. The scheme requires that changes in synaptic weight take place on a time scale that is fast enough to adapt to single wave propagation. The anti-Hebbian synaptic weight adaptation response to an active and inactive presynaptic and postsynaptic cell for a range of $R$ values is shown in Figure 4. A synaptic adaptation rate of 10 is used in the adaptive model so that the synaptic connections adapt to the activity level of the cortex on a time scale consistent with the propagation of model waves.

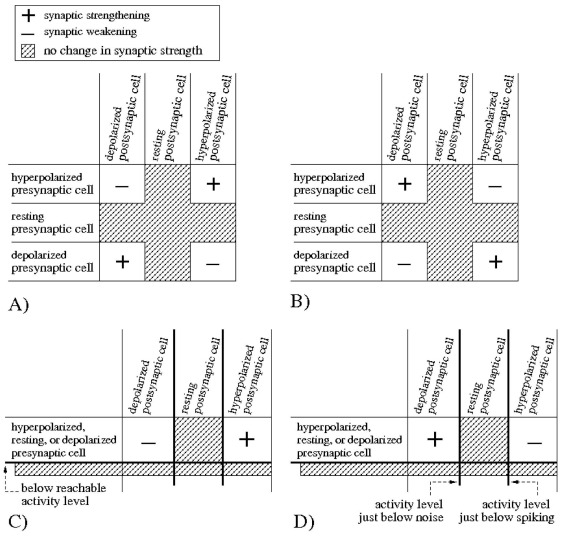


Fig. 2. Hebbian and anti-Hebbian adaptation paradigms. Changes in synaptic strength are represented in the Hebbian (A) and anti-Hebbian (B) learning rules. Postsynaptic Hebbian and anti-Hebbian learning rules are represented in (C) and (D) respectively.

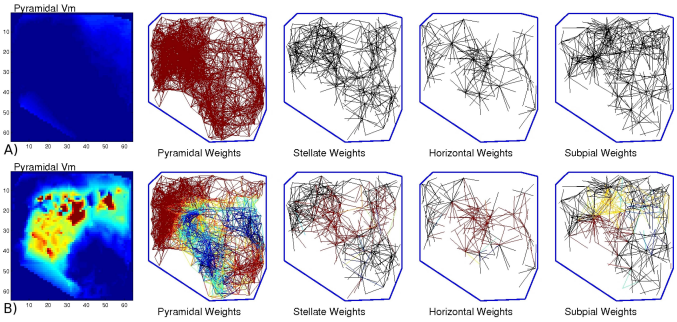


Fig. 3. Pyramidal cell activity state and corresponding pyramidal-to-pyramidal, stellate-to-pyramidal, horizontal-to-pyramidal, and subpial-to-pyramidal synaptic weight states. Both pyramidal cell activity levels and synaptic weight values are coded on a blue (low) to red (high) scale. Ten percent of the total number of synaptic connections are shown. Top row: Model hyperpolarized state following a wave propagation. Bottom row: Model state during a propagation wave.

### C. Data Analysis

Responses of the model to simulated visual stimuli were recorded as $Matlab$ movies. The movies represented a triangle-based linear interpolation of the activity of non-uniformly spaced pyramidal cells over a uniformly spaced grid covering the model space (leftmost frames of Figure 3) at each simulation time step. The movies were analyzed using a two-step Karhunen-Loeve decomposition to project each movie onto a three dimensional space that retains both spatial and temporal dynamics of the model waves. This processes is described in detail by Nenadic *et al.* [7] and Du *et al.* [14], [15].

## III. Wave Generation in the Non-adaptive and Adaptive Models

### A. Non-adaptive Model

Figure 5-A shows the response of the large-scale model with subpial cells, but without synaptic adaptation, to activation

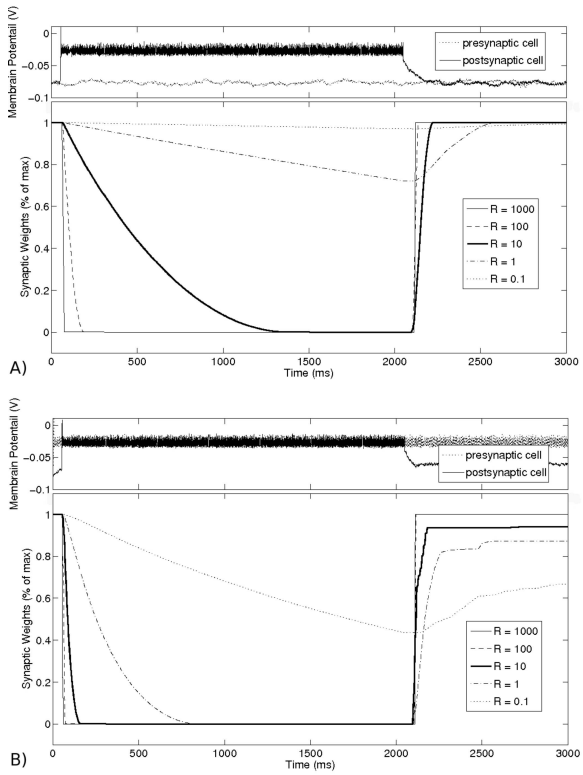


Fig. 4. Anti-Hebbian synaptic weight response to pre-synaptic and post-synaptic activity for a range of adaptation rate values. This figures shows the membrane potentials of a presynaptic and postsynaptic neuron and the changes in synaptic weights between those two neurons for several values of the adaption rate (R). A. Synchronized activity in the presynaptic and postsynaptic cells. B. Unsynchronized activity in the presynaptic and postsynaptic cells.

of the 20 neurons at the right end of the row of geniculate neurons. The top row of Figure 5-B shows a wave generated by activating the 20 neurons at the left end of the row of geniculate neurons. The general features of the waves are the same in both cases. Both stimuli evoke a wave at the rostral pole of the cortex that propagates across the cortex to its caudal pole. It then subsides and is followed by a long-lasting after-hyperpolarization. These cortical responses can be divided into four phases for descriptive purposes. The *initiation phase* extends from the first appearance of the initial depolarization to the point in time at which the wave begins to propagate. The *propagation phase* extends from the time at which the wave begins to propagate to the time at which it begins to subside. The *cessation phase* extends from the time at which the wave begins to subside to the end of the depolarization. The *after-hyperpolarization phase* is a long-lasting period of hyperpolarization that follows wave cessation. As exemplified by the bottom row of Figure 5-B, even a full 2 seconds after an initial wave the after-hyperpolarization is still present enough to prevent the model from producing a second wave in response to a second input pulse. The large-scale model without synaptic adaptation, thus, does not respond to repetitive stimuli at a realistic time scale.

### *B. Responses to Repetitive Stimuli in the Adaptive Model*

By contrast, the adaptive model does respond to repetitive stimuli. Figure 6-A shows the pyramidal cell responses to repeated strong stimulation of the left edge of the row of geniculate neurons. As is indicated by this example, in some cases a strong stimulation causes the inhibitory response to suppress the wave during the propagation phase. However, the adaptive weight response to the resulting after-hyperpolarization phase leads to rapid propagation of the second stimulus wave ($2^{nd}$ row of Fig. 6-A). As the pulses continue, the model remains responsive to the stimuli despite the after-hyperpolarization phase after each wave. Details of the repetitive responses can be seen by plotting the average membrane potentials of all of the cells in the model as a function of time over 10 simulations of 10 waves (Fig. 7-A). It can be seen by the average membrane potentials in Figure 7-A and the darker blue colors indicating lower pyramidal cell membrane potentials in Figure 6-A that the after-hyperpolarization phase leaves the cortex in a lower activity state after a wave, as opposed to before a wave. In response to this, the adaptation scheme causes the synaptic weights of the adapting synapses to be driven past their original values in response to the after-hyperpolarization phase. As multiple waves propagate, the after-hyperpolarization phase and the corresponding synaptic adaptation becomes more and more pronounced. This progression continues until a lower bound on the pyramidal hyperpolarization is reached. This occurs after 5 to 6 waves in the adaptive-model. Once the lower bound of the after-hyperpolarization phase is reached, the activities of the pyramidal cells before and after a wave consistently give rise to a steady state periodic response in terms of total model pyramidal cell activity. The activity patterns of the waves also seem to reach a steady state. The first 4 to 5 responses can show considerable variation in wave patterns. As exemplified by row 3 of Figure 6-A, rebound waves similar to those observed by Wang et. al. [9] that propagate back from the caudal pole to the rostral pole of the cortex may be seen in the first 3 to 4 waves. However, as the average activity patterns of 10 waves produced by a $6^{th}$ input pulse and a $10^{th}$ input pulse (Fig, 6-B) and the response wave of a $20^{th}$ input pulse (Fig. 6-C), demonstrate the propagation pattern response to identical input pulses also reaches a steady state after 5 to 6 waves in the adaptive model. Likewise, the synaptic weights also reach a steady state periodic response in response to the cyclic pyramidal activity (Fig. 7-B).

Another consequence of the progression to the steady state is a shortening of the total duration of a wave. As is illustrated in Figure 8-A, this is due mostly to an initial shortening of the propagation phase and a shift to a pro-activity state due to the after-hyperpolarization phase of the previous wave. This allows the pyramidal cell activity to grow faster. The shift back to the anti-activity state of the model is less pronounced in response to the shortened burst of propagation activity. Thus, the second and third waves result in longer cessation phases compared to the cessation phase after the first wave. The after-hyperpolarization phases become more pronounced as the model progresses further towards the steady state, which slows the building of wave activity in the initiation phase slightly.

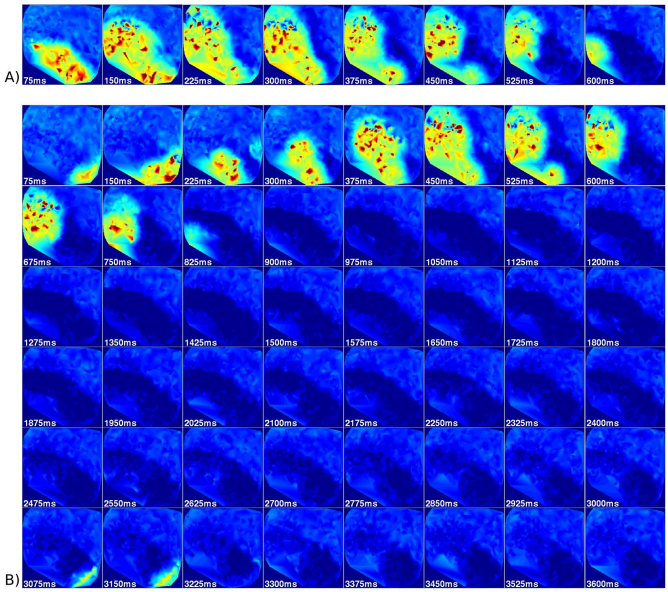


Fig. 5. Responses of the non-adaptive model with subpial cells to right and left stimuli. A. Eight frames at 75, 150, 225, 300, 375, 450, 525, and 600 ms from a simulation with a strong 150 ms input pulse to the 20 rightmost LGN cells at 0 ms. B. Forty eight frames at 75 ms intervals from a simulation with a strong 150 ms input pulse to the 20 rightmost LGN cells at 0 and 3000 ms.

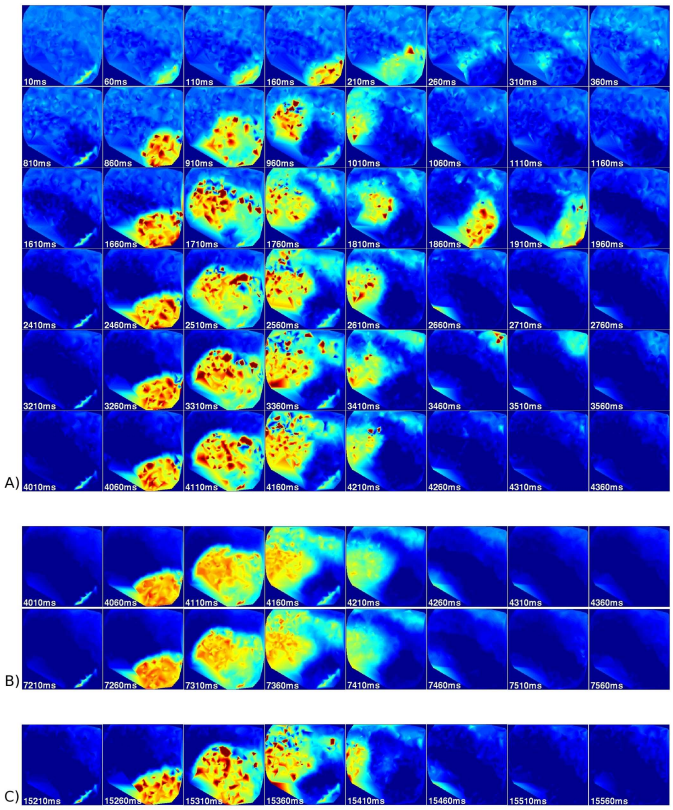


Fig. 6. Response of the adaptive model to consecutive 150 ms left pulses at 800 ms intervals. A. Example of first six activity responses. Each row shows eight activity frames depicting the response at 10, 60, 110, 160, 210, 260, 310, and 360 ms after a single input pulse. Thus, the top row shows responses at 10 ms to 360 ms following a pulse at 0 ms. The second row shows the response at 820 ms to 1,160 ms following a single pulse at 800 ms, and so forth for rows three to six. B. The average response patterns over ten simulations of ten consecutive input pulses for the sixth (top row) and tenth (bottom row) pulses. C. Activity response to the twentieth left input pulse.

However the stronger after-hyperpolarization also leads to even stronger pro-activity states preceding the next geniculate stimulus and the strength of the wave activity is increased as a result of progressively stronger pro-activity states. This causes more pronounced wave activity bursts that last slightly longer and the shift back to the anti-activity state following the wave becomes more pronounced. This accounts for the re-shortening of the cessation phase. The wave phase duration time eventually reach a steady state when the strengthening wave activity and increasing after-hyperpolarization reach their bounds, and a balance with the resulting stronger pro-activity states is achieved.

### *C. Habituation to Continuous Stimuli in the Adaptive Model*

Similar to their response to repeated stimuli (Fig 5), the non-adaptive models respond to continuous stimuli with one initial wave despite the continued presence of an input stimulus. However, flashes of pyramidal cell activity do occur in the area covered by the geniculate axons after the cessation phase of the initial wave. It could be expected that these flashes would result in new waves in the adaptive model just as periodic inputs result in multiple waves. However, the cortex responds with a single initial wave lasting about 300 ms to a sustained 12 nA input to 20 geniculate neurons for 1,000 ms. The initial wave is followed by sustained activity in the area directly stimulated by the center 20 neurons, but this activity does not lead to the development of a wave. Multiple waves do not occur unless the stimulus is removed and then reapplied, as it was in the periodic input simulations of section III-B. A closer look at the weight state of the model in this sustained localized activity state reveals the reason for this lack of wave response. The connections to the pyramidal cells most directly stimulated by the geniculate inputs do not returned to the steady state. This is due to the continued activity of these postsynaptic pyramidal cells, which prevents synapses from adapting back to the original values. These pyramidal cells must first become inactive to facilitate the adaptive response. This can be accomplished by either removing the stimulus, as in the periodic case, or shifting the stimulus to geniculate neurons that stimulate other areas in the model. Shifting the input stimulation to reach pyramidal cells outside of the unadapted area quickly leads to building activity and wave propagation. Thus, the adaptive model remains responsive to changing stimuli and becomes unresponsive to unchanging stimuli.

## IV. Stimulus Discrimination in the Adaptive-Model

A key feature of the non-adaptive model is that spatially distinct stimuli lead to statistically distinct features in activity waves that can be used to discriminate between visual targets. Du *et al.* [14], [15] carried out simulations in which spots of light positioned at the left edge, center, and right edge of the horizontal meridian of visual space were simulated. Left, center and right spots of light were modeled as 150 ms square pulse stimuli to groups of 20 geniculate neurons at the left

edge, center, and right edge of the array of geniculate neurons. Ten simulations of six randomly generated left, center, and right inputs with the same parameters used by Du *et al.* [14] were used to generate five model waves at 800 ms intervals to allow the model to reach the steady state described in section III-B. Both the cellular activity levels of all model cells and the weight values for all model synaptic connections at the time of completion of the simulation were recorded and averaged over the ten simulations. These values were then taken as the values for the steady state discussed in section III-B and used as the initial conditions for the simulations of the left-center-right task analysis of the adaptive model. Twenty simulations of two consecutive waves initiated at 0 and 600 ms for each possible pairing of first and second left, center, and right stimuli were run. This resulted in 60 first left, 60 first center, and 60 first right waves and 60 second left, 60 second center, and 60 second right waves for analysis.

The cortex waves for the three input locations were projected onto a three dimensional detection space using a two-step Karhunen-Loeve decomposition (Nenadic *et al.* [7] and Du *et al.* [14], [15]) and detection was done using the discrimination boundaries in this space. The detection error plots (Fig. 8-A) show that the left, center, and right waves remain highly distinguishable up to the end of the cessation phase. The detection plane clusters for each input type become less dense over time as the waves propagate for both the non-adaptive and adaptive model, and eventually begin to overlap during the cessation phase resulting in some detection error. Very small differences between detection plane points during the initiation phases, due to the fact that all model waves originate in the rostral pole, are compensated for by even smaller differences between points of the same input location during the initiation phase. The adaptive model compares favorably to the non-adaptive model both in terms of input location detection despite the shortened wave durations and resulting propagation phase overlap between left, center, and right waves. In fact, a case can be made that the presence of a strong afterhyperpolarization phase once the steady state has been reached serves to suppress the noise activity of the model and sharpen the spatial differences between the waves, more than adequately compensating for the decreased temporal differences between the waves.

Nenadic *et al.* [7] showed that the non-adaptive model was able to discriminate the speeds at which simulated spots move along the array of geniculate neurons. Du *et al.* [15] subsequently confirmed this result using a sliding time window representation of the wave. The ability of the adaptive-model to distinguish moving stimuli was evaluated using stimuli moving in separate directions at different speeds. Since the center of the array of geniculate neurons corresponds to the center of the visual field, stimuli originated at the center of the array of geniculate neurons and this task is referred to as the center-out task. Simulations were run with the model starting at the steady state cellular activity and synaptic weight values. They involved two consecutive stimulus patterns resulting in two separate waves. The first and second waves were produced by four input types of fast and slow shifting blocks of 20 geniculate neurons towards the caudal/left (position 1) or rostral/right (position 201) pole of the row of geniculate neurons. Stimulus speed depended on the rate at which the inputs were shifted along the row of geniculate neurons. Fast and slow rates shifted the inputs one position in the row every 1.24 ms and 2.5 ms, respectively. For a slow shift to the right, for example, the inputs were at positions 91 to 110 (the middle 20 positions) in the row at simulation time 0 ms and were then the shifted to positions 92 to 111 at time 2.5 ms, and so on, until the input block was at position 201. It took 137.5 and 275 ms to move the inputs from the center to the end of the row of geniculate neurons for the fast and slow rates, respectively. Twenty simulations each of the four shifting stimulus types (center-to-left, slow, center-to-right slow, center-to-left fat, and center-to-right fast) were run. Because there are four input stimulus types in the center-out task, linear log-likelihood boundaries can not be drawn in the three dimensional detection space. However, maximum log-likelihood ratios for each position in the detection space can be calculated and used for detection. As is indicated by the detection error rates of the first and second waves (Figure 8-B) the overlap of the input type clusters in the detection space remains small. In fact, the detection error rates of the center-out task are very comparable to those of the left-center-right task indicating the adaptive models ability to distinguish stimulus differences in motion as well as location.

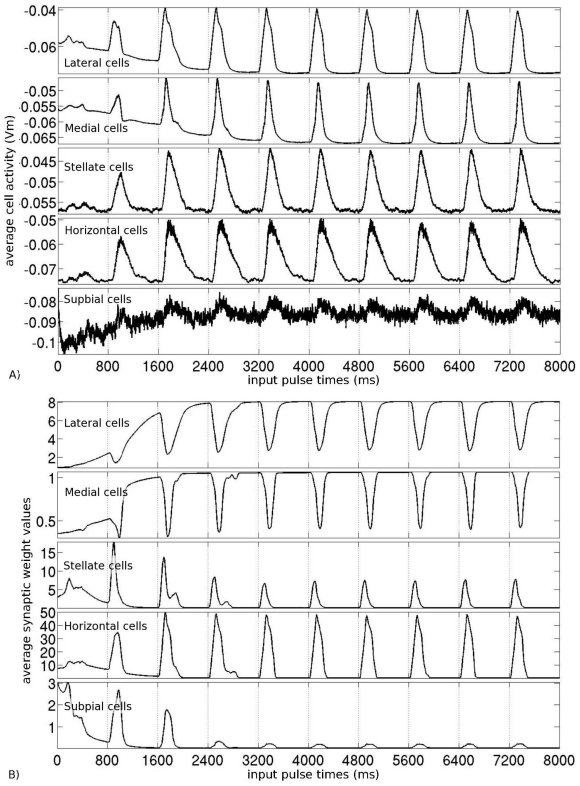


Fig. 7. A. Average membrane potentials for each type of cell for ten waves. B. Average weights of all incoming synapses for each cell type over 10 waves propagations. Weights were sampled every 100 ms. The vertical lines indicate the start times of 150 ms left input pulses.

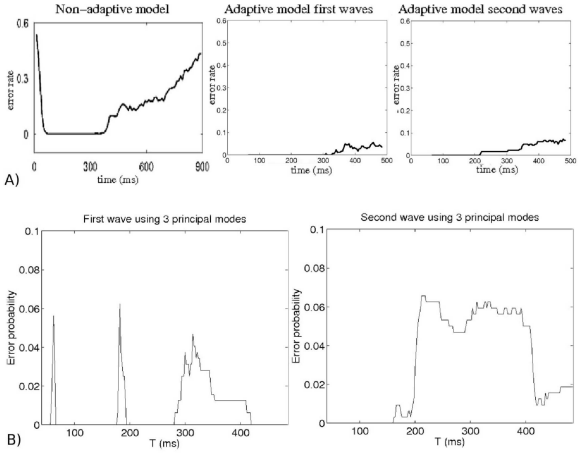


Fig. 8. A. Error rates over time for first vs. second stationary stimuli waves. All plots use a w of 10 and a SDW of 55 ms. Left: Detection error probability over time for non-adaptive cortex [14]. Center: Error rate over time for the set of first waves. Right: Error rate over time for the set of second waves. B. Error rates over time for the center-out task. Right: detection error rates using the all three B- dimensions for the first waves. Left: detection error rates using all three B-dimensions for the second waves.

## V. Discussion

### A. Synaptic Plasticity

Hebb [17] formalized a rule governing how synaptic effectiveness could change as a function of activity in the presynaptic and postsynaptic activities elements of synapses. He postulated that synaptic strength should increase when activity in the presynaptic element of the synapse resulted in activity of the postsynaptic element. An experimental test of Hebb's postulate came with the discovery of long term potentiation (LTP) in rat hippocampus [18]. (See the review by Lynch [19].) Subsequent work (see the review by Bear and Abraham [20]) has demonstrated the existence of the opposite effect, long term depression (LTD), in a variety of synapses. In LTD, correlated activity in the presynaptic and postsynaptic elements results in a weakening of the synapse. The cellular mechanisms underlying LTP and LTD can be very complex (see the recent review by Malenka and Bear [21]), but one common mechanism involves the influx of calcium through the activation of NMDA receptors on the postsynaptic cell and the engagement of specific intracellular signaling cascades that result in either the upregulation or downregulation of NMDA receptors in the postsynaptic cell. A recently discovered form of synaptic plasticity is Anti-Hebbian learning, which involves the increased effectiveness of a synapse when firing in the presynaptic and postsynaptic elements are not correlated. Anti-Hebbian learning was first described in the electrosensory lobe of electric fish [22], and has since been described in a variety of neurons, including inhibitory interneurons in the hippocampus [23]. Anti-Hebbian learning appears to involve calcium permeable AMPA receptors, instead of NMDA receptors [23]. Both Hebbian and anti-Hebbian learning are forms of long term synaptic plasticity. However, many forms of short term synaptic plasticity (see Zucker and Regehr [24]) are known. It is well established that the various forms of synaptic plasticity are cell-specific, so that different populations of neurons in a given structure can show different forms of plasticity (e.g. Lu *et al.*,[25], Patenaude *et al.* [26]). Two forms of synaptic plasticity were incorporated into our large-scale model of turtle visual cortex in this paper.

Synaptic plasticity was incorporated in synapses between pyramidal cells using an anti-Hebbian learning rule. The synapses between pyramidal cells are known to be glutaminergic and to access both AMPA and NMDA receptors. Kriegstein and Connors [27] described a form of short term plasticity, paired-pulse facilitation, in pyramidal cells in turtle visual cortex that peaked with interpulse intervals of approximately 100 ms. LTP or LTD have so far not been described in turtle visual cortex, but several studies indicate that both LTP and LTD do occur in turtles and likely involve cellular mechanisms similar to those described in other species. Muoz *et al.* [28] showed that tetanic stimulation of the septum produces LTP in the limbic cortex of turtles. The potentiation is blocked by NMDA receptor antagonists and by nifedipine, an antagonist of L-type calcium channels. Johnson and Mitchell [29] showed the presence of LTD in motoneurons innervating the pectoralis muscles of turtles. Keifer and her colleagues [30], [31], [32], [33], [34], [35] have shown that a Hebbian-like conditioning of the eye blink reflex exists in an *in vitro* brainstem preparation of turtles. Pairing stimulation of the auditory nerve with stimulation of the trigeminal nerve produces a conditioned eyeblink response that is dependent upon NMDA receptors. Conditioning reduces immunoreactivity to the calcium binding protein, calbindin-D28K, in the abducens motoneurons responsible for the eyeblink. Anti-Hebbian learning has not been demonstrated in turtle visual cortex.

Synaptic plasticity was incorporated in the model in the synapses between the three types of inhibitory interneurons and pyramidal cells using a Hebbian learning rule. Inhibitory synapses in turtle visual cortex are known to be GABAergic and to access both $GABA_A$ and $GABA_B$ receptors (e.g. [27]). Synaptic plasticity has been studied principally in excitatory glutaminergic synapses. However, recent work has demonstrated several forms of long-term plasticity in inhibitory synapses in several structures, including the hippocampus, neocortex and cerebellum [36], [37], [26]. The mechanisms underlying LTP and LTD in inhibitory synapses are not as well characterized as are those of glutaminergic synapses, and there have been no studies of plasticity in inhibitory synapses in turtles. The incorporation of a Hebbian learning rule in the model for inhibitory synapses is plausible, based on what little is known of the plasticity of inhibitory synapses in mammals.

### B. Modeling Hebbian Learning

Mathematical models of Hebbian learning can be divided generally into biophysical models, which attempt to capture the cellular details of synaptic plasticity, and phenomenological models, which represent the general effects of plasticity (e.g. [38]). Given the poor level of information about the cellular mechanisms underlying synaptic plasticity in turtle visual cortex, we elected to use a simple phenomenological model of Hebbian and anti-Hebbian learning. (See Haykin [39] and Gerstner and Kistler [40] for recent discussions of models

of Hebbian learning.) Both learning rules used the membrane potentials of the presynaptic and postsynaptic neurons. They are essentially correlation models in which the rate of change in synaptic weight depends upon the membrane potentials of the two cells relative to a threshold window. The use of the window, as opposed to simply using the resting membrane potential, as a reference point allowed a noise current to be included in the neurons. The learning rules are variants of rate dependent rules (see Gerstner and Kistler [40]) and are relatively crude approximations of synaptic plasticity because it is now well-established that plasticity typically depends upon the timing between the presynaptic and postsynaptic spikes in the two neurons (reviews: Dan and Poo [41], [42]). Learning windows can be measured experimentally, but these measurements have not been done for neurons in turtle visual cortex. Consequently, no effort was made to include timing effects in our large-scale model at this time.

### *C. Functional Significance of Adaptation in Turtle Visual Cortex*

Our large-scale model of turtle visual cortex captures the basic features of the waves generated in real turtle cortex by single stationary or moving visual stimuli. However, the model cortex does not respond to repeated visual stimuli because the waves are followed by a long-lasting period of hyperpolarization due to the activity of $GABA_B$ receptors in neurons postsynaptic to inhibitory interneurons. The strengths of the $GABA_B$-receptors were chosen by trial and error to produce a wave response. Too little $GABA_B$ inhibition results in waves that do not subside or stay in the cessation phase a unrealistic length of time. As indicated, stronger $GABA_B$ inhibition leads to the long lasting after-hyperpolarization phase following wave cessation. Because no data on miniature $GABA_B$-receptor mediated currents are available the conductances were constrained using the time course of slow IPSPs [8]. Using too fast of a $GABA_B$-receptor time course causes the $GABA_B$ inhibition to react too soon and like the case of too little $GABA_B$ inhibition when the wave reaches the waves do not subside. A slower $GABA_B$-receptor time course causes the after-hyperpolarization to last even longer. It should be noted that the time coarse can be shortened to the point where a second wave is seen if the simulation is run long enough, but no time course was found that caused the initial wave to subside and allowed for a seconded wave within 1000 ms of the first wave.

The adaptive model developed in this paper presents a possible mechanism by which small inputs that occur during the afterhyperpolarization-phase of wave propagation can lead to the generation of new waves. It uses a balance of Hebbian and anti-Hebbian synaptic plasticity to overcome the afterhyperpolarization present in the non-adaptive forms of the model. As reviewed above, the cellular mechanisms underlying synaptic plasticity in turtle visual cortex are not known, so the simulations described in this paper demonstrate that incorporating some form of synaptic plasticity in the model is sufficient to allow the model cortex to respond to repetitive stimuli without specifying the exact forms of plasticity that are required.

Gusel'nikov and Pivavarov [10] showed that neurons in turtle visual cortex habituate to repeated presentations of a stimulus at a specific point in visual space, but then respond robustly to a different stimulus presented at the same point. This paper demonstrates that Hebbian and anti-Hebbian forms of plasticity are sufficient to account for this phenomenon. The effect is due to the continued activity of the pyramidal cells that receive inputs from the subset of geniculate afferents that are activated by the repetitive stimulus. This activity prevents synapses from adapting back to their original values. The pyramidal cells must first become inactive to facilitate the adaptive response. This can be accomplished by either removing the stimulus, as in the periodic case, or shifting the stimulus to geniculate neurons that stimulate other areas in the model.

An important feature of waves in both the real and non-adaptive model cortices is that the spatiotemporal dynamics of the waves contain information about the positions and speeds of visual stimuli. The information content of waves in the adaptive model was studied using left/center/right stimuli and a center out task using moving stimuli. Our results indicate that waves in the adaptive model contain information about the properties of the stimulus. A quantitative difference between the non-adaptive and adaptive models is that the maximum information about the stimulus occurs during the initiation phase in the adaptive models. However, good stimulus discriminability extends into the propagation phase in the adaptive model.

## VI. Conclusion

Our large-scale model of turtle visual cortex accurately captures the spatiotemporal dynamics of the responses of the real cortex to flashes of light or to moving stimuli. However, the real turtle cortex shows responses to repeated stimuli that are not present in the model. The principal result of this study is that the model cortex can show responses to repeated stimuli if a form of synaptic plasticity is incorporated into the cortex using Hebbian and anti-Hebbian learning rules.

## References

[1] J. C. Prechtl, "Visual motion induces synchronous oscillations in turtle visual cortex.", *Proc Natl. Acad. Sci.*, vol. 91, pp. 12467 - 12471, 1994.

[2] J. C. Prechtl, L. B. Cohen, B. Pesaran, P.P. Mitra and D. Kleinfeld, "Visual stimuli induce waves of electrical activity in turtle cortex.", *PNAS*, vol. 94, pp. 7621 - 7626, 1997.

[3] J. C. Prechtl, T. H. Bullock and D. Kleinfeld, "Direct evidence for local oscillatory current sources and intracortical phase gradients in turtle visual cortex.", *PNAS* , vol. 97, pp. 877 - 882, 2000.

[4] D. M. Senseman, "Spatiotemporal structure of depolarization spread in cortical pyramidal cell populations evoked by diffuse retinal light flashes.", *Vision Neuroscience*, vol. 16, pp. 65-79, 1999.

[5] D. M. Senseman and K. A. Robbins, "Modal behavior of cortical neural networks during visual processing.", *J. Neurosci.*, vol. 19 RC3, 1999.

[6] D. M. Senseman, and K. A. Robbins, "High-speed VSD imaging of visually evoked cortical waves; decomposition into intra- and intracortical wave motions.", *J. Neurophysiol.*, vol. 87, pp. 1499-1514, 2002.

[7] Z. Nenadic, B. K. Ghosh, P. S. Ulinski, "Modeling and estimation problems in the turtle visual cortex.", *IEEE Trans. on Biomedical Engineering*, vol. 49(8), pp. 753-762, 2002.

[8] Z. Nenadic, B. K. Ghosh, P. S. Ulinski, "Propagating waves in visual cortex: A large-scale model of turtle visual cortex.", *IEEE J. of Comp. Neurosci.*, vol. 14, pp.161-184, 2003.

[9] W. Wang, C. Campaigne, B. K. Ghosh, and P. S. Ulinski, "Two cortical circuits control propagating waves in visual cortex.", *J. of Comp. Neurosci.*, vol. 19, pp. 263-289, 2005.

[10] V. I. Gusel'nikov and A. S. Pivovarov, "Postsynaptic mechanism of habituation of turtle cortical neurons to moving stimuli.", *Neuroscince and Biology*, vol. 9 (1978), translated from Vysshei Nervnoi Deyatel'nosti, vol. 6 No. 5, pp. 1082-1090, 1976.

[11] J. C. Prechtl and T. H. Bullock, "Plurality of visual mismatch potentials in a reptile.", *J. Cognitive Neurosci.*, vol. 5, pp. 177-187, 1993.

[12] J. C. Prechtl and T. H. Bullock, "Event-related potentials to omitted visual stimuli in a reptile.", *Electroencephal. Clinical Neurophysiol.*, vol. 91, pp. 54-66, 1994.

[13] J. M. Bower and D. Beeman, *The Book of Genesis: Exploring Realistic Neural Models with General Neural Simulation System.*, Second Edition, New York, Springer-Verlag, 1998.

[14] X. Du, B. K. Ghosh, and P. S. Ulinski, "Encoding and decoding target locations with waves in the turtle visual cortex.", *IEEE Trans. on Biomedical Engineering*, vol. 52[4], pp. 566-577, 2005.

[15] X. Du, B. K. Ghosh, and P. S. Ulinski, "Encoding of motion targets by waves in turtle visual cortex.", *IEEE Trans. on Biomedical Engineering*, vol. 53[8], pp. 1688-1695, 2006.

[16] W. Wang, S. Luo, B. K. Ghosh, and P. S. Ulinski, "Generation of receptive fields of subpial cells in turtle visual cortex.", *J. of Integrative Neurosci.*, vol. 5(4), pp. 561-593, 2006.

[17] D. O . Hebb, The Organization of Behavior., John Wiley and Sons, New York, 1949.

[18] T. V. P. Bliss and T. Lomo, "Long-lasting potentiation of synaptic transmission in the dentate area of the anaesthetized rabbit following stimulation of the perforant path." *J. Physiol.*, vol. 232, pp. 331-356, 1973.

[19] M. A. Lynch, "Long-term potentiation and memory." *Physiol. Rev.*, vol. 84, pp. 87-136, 2004.

[20] M. F. Bear and W. C. Abraham , "Long-term depression in hippocampus.", *Ann. Rev. Neurosci.*, vol. 19, pp. 437-462, 1996.

[21] R. Malenka and M. Bear, "LTP and LTD: an embarrassment of riches". *Neuron*, Vol. 44(1), pp. 5-21, 2004.

[22] C. Bell, V. Han, Y. Sugawara and K. Grant, "Synaptic plasticity in a cerebellum-like structure depends on temporal order.", *Nature*, vol. 387, pp. 278-281, 1997.

[23] D. M. Kullman and K. Lamsa, "Roles of distinct glutamate receptors in induction of anti-Hebbian long-term potentiation.", *J. Physiol (Lond.)*, vol. 586, pp. 1481-1486, 2008.

[24] R. S. Zucker and W. G. Regehr, "Short-term synaptic plasticity.", *Ann. Rev. Physiol.*, vol. 64, pp. 355-405, 2002.

[25] J-T. Lu, C. Li, J-P., Zhao, M. Poo and X. Zhang, "Spike-timing-dependent plasticity of neocortical excitatory synapses on inhibitory interneurons depends on target cell type.", *J. Neurosci.*, vol. 27, pp. 9711-9720, 2007.

[26] C. Patenaude, G. Massicotte, and J-C. Lacaille, "Cell-type specific GABA synaptic transmission and activity-dependent plasticity in rat hippocampal stratum radiatum interneuronss.", *Europ. J. Neurosci.*, vol 22, pp.179-188, 2005.

[27] A. R. Kriegstein and B. W. Connors, "Cellular physiology of the turtle visual cortex: synaptic propoerties and intrinsic circuitry", *J. of Neurosci.*, vol. 6[1], pp. 178-191, 1986.

[28] M. D. Muoz, J. M. Gaztelu, and E. Garca-Austt, "Homo- and heterosynaptic long-term potentiation in the medial cortex of the turtle brain in vitro", *Brain Research*, vol. 807, pp. 155-159, 1998.

[29] S. M. Johnson and G. S. Mitchell, "Activity-dependent plasticity of descending synaptic inputs to spinal motoneurons in an in vitro turtle brainstem-spinal cord preparation.", *J. Neurosci.*, vol. 20, pp. 3487-3495, 2000.

[30] J. Keifer, "In vitro eye-blink reflex model: role of excitatory amino acid receptors and labeling of network activity with sulfarhodamine.", *Exp. Brain Res.*, vol. 97, pp. 239-253, 1993.

[31] J. Keifer, "In vitro eye-blink classical conditioning is NMDA receptor dependent and involves redistribution of AMPA receptor subunit GluR4.", *J. Neurosci.*, vol. 21, pp. 2434-2441, 2001.

[32] J. Keifer and T. G. Clark , "Abducens conditioning in in vitro turtle brainstem without cerebellum requires NMDA receptors and involves upregulation of GluR4 contaiing AMPA receptors.", *Exp. Brain Res.*, vol. 151, pp. 405-410, 2003.

[33] J. Keifer, B. T. Brewer, P. E. Mehan, R. J. Brue and T. G. Clark, "Role for calbindin-D28K in in vitro classical conditioning of abducens nerve responses in turtles.", *Synapse, vol.* 49, pp. 106-115, 2003.

[34] J. Keifer and M. Mokin, "Distribution of anterogradely labeled trigeminal and auditory nerve boutons on abducens motor neurons in turtles: Implications for in vitro classical conditioning.", *J. Comp. Neurol.*, vol. 471. pp. 144-152, 2004.

[35] M. Mokin and J. Keifer , "Targeting of GluR4-containing AMPA receptors to synaptic sites during in vitro classical conditioning.", *Neruosci.*, vol. 182, pp. 219-228, 2004.

[36] V. Chevaleyre and P. E. Castillo, "Heterosynaptic LTD of hippocampal GABAergic synapses: A novel role of endocannabinoids in regulating excitability.", *Neuron*, vol. 38, pp. 461-472, 2003.

[37] J-L. Gaiasara, O. Caillard and Y. Ben-Ari, "Long-term plasticity at GABAergic and glycinergic synapses: mechanisms and functional significance.", *Trends Neurosci.*, vol. 25, pp. 564 - 570, 2002.

[38] Q. Zou and Desthexhe, "Kinetic models of spike-timing dependent plasticity and their functional consequences in detecting correlations.", *Biol. Cybernetics*, vol. 97, pp. 81-97, 2007.

[39] S. Haykin, Neural Networks: A Comprehensive Foundation, Second Edition, New Jersey, Prentice-Hall Inc., 1999, chapter 2, pp. 55-58.

[40] W. Gerstner and W. M. Kistler, "Mathematical formulations of Hebbian learning.", *Biol. Cybernetics*, vol. 87, pp. 404-415, 2002.

[41] Y. Dan and M. Poo , "Spike-timing-dependent plasticity of neural circuits.", *Neuron*, vol. 44, pp. 23-30, 2004.

[42] Y. Dan and M. Poo, "Spike timing-dependent plasticity: From synapse to perception.", *Physiol. Rev.*, vol. 86, pp. 1033-1048, 2006.

**Zachary V. Freudenburg** received the M.S. degree in Computer Science from the University of Groningen in the Netherlands and his B.S. degree in Physics from Beloit College, Beloit, WI. Zachary is currently working toward the PhD degree in Computer Science at the Department of Computer Science and Engineering at Washington University, St. Louis, MO. His research interests include complex neurological system modeling, brain computer interface development, and real time high dimensional data clustering techniques.

**Bijoy K. Ghosh** received the B. Tech and M.Tech degrees in Electrical and Electronics Engineering from BITS, Pilani, the Indian Institute of Technology, Kanpur, India and the PhD degree in Engineering from the Decision and Control Group of the Division of Applied Sciences, Harvard University, Cambridge, MA in 1977, 1979 and 1983, respectively. From 1983 to 2006, he was with the Department of Electrical and Systems Engineering, Washington University, St. Louis, MO, where he was a Professor and Director of the Center for BioCybernetics and Intelligent Systems. Currently he is the Brooks Regents Professor of Mathematics and Statistics at Texas Tech University, Lubbock. His research interests are in multivariable control theory, machine vision, biomechanics and control. Bijoy is a 1988 recipient of the Donald P. Eckmann award from the American Automatic Control Council and is a Fellow of the IEEE. He also received the JSPS invitation fellowship in the year 1997.

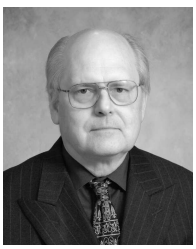

**Philip S. Ulinski** received the Ph.D. degree in Zoology from Michigan State University, East Lansing, MI, 1968. He is currently Professor Emeritus in Computational Neuroscience at the University of Chicago, Chicago, IL. His research interests include the functional organization of the cerebral cortex and computational models of neural circuits.